

Micromotor That Carries Its Own Fuel Internally

Ruo-Yu Dong,^{||} Yifan Zhang,^{||} Kai Lou, and Steve Granick*



Cite This: *Langmuir* 2020, 36, 7701–7705



Read Online

ACCESS |

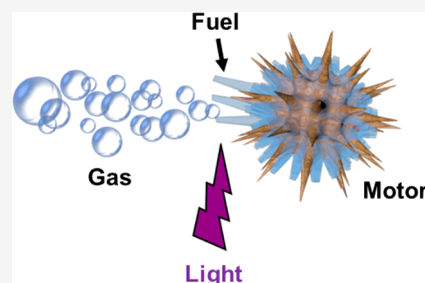


Metrics & More



Article Recommendations

ABSTRACT: Micromotors enjoy burgeoning interest but a limitation of their design is to require continuous supply of new fuel. The preponderance of extant micromotors depend, for their motion, on irradiation by light or exposure to acid in their environment. Here we demonstrate a motor that carries its own fuel internally, in this sense representing an analogue, in micron-sized objects, of the internal combustion engine. The fuel is DPCP (diphenylcyclopropenone) microcrystal, a solid-state chemical that after ignition by UV light requires no further irradiation to sustain a chemical reaction that emits carbon monoxide gas that can be used to propel the particle on which this chemical resides. It is loaded asymmetrically onto inexpensive microparticles to produce internally fueled propulsion with speed up to $\sim 20 \mu\text{m/s}$ over distances up to 15 times the capsule length in water. Once ignited, the motors maintain their direction of motion and move without need for light to follow their path. Possible strategies to extend the idea beyond the current proof of concept are discussed.



■ INTRODUCTION

Particles that self-propel, “micromotors”, constitute one of the most rapidly growing sectors of modern microengineering.^{1–3} Excitement for this concept is driven partly by a myriad of potential applications, from targeted cargo delivery to biosensing and environmental remediation.^{4,5} To achieve self-propulsion, the current frequent design is to use surface catalytic reactions to harvest propulsion energy from the surface environment, for example, use of chemical reactions triggered by light⁶ or pH⁷ stimuli. However, a limitation is that such motors require continuous presence of their trigger and consume fuel from the surroundings to maintain self-propulsion, which restricts their application scenarios. For example, a widely used propulsion method is metal-catalyzed decomposition of hydrogen peroxide triggered by UV/visible light,^{8–11} and there exist other chemistries that are analogous in that they require continuous stimulus from the environment.^{12–15} Micromotors, when they are subject to this limitation, cannot navigate beyond reach of the propulsion stimulus. This study reports our progress to design micromotors that run on internal fuel instead.

A schematic diagram of the concept is shown in Figure 1A. As we implement the approach here, propulsion is based on the decarbonylation of DPCP (diphenylcyclopropenone) into DPA (diphenylacetylene) and CO (carbon monoxide) gas, initiated by UV light irradiation (Figure 1B). The DPCP crystals present a solid-state fuel, attached to the motor surface. The microparticle was selected to be inexpensive yet with a spiky “hedgehog” surface morphology, as sharp needles are known to impede particle aggregation.¹⁶ Naturally occurring sporopollenin exine capsules¹⁷ meet these requirements.

Extracted from sunflower pollen grains, these particles have attractive features as candidates for motor carriers, as they are biocompatible, nontoxic, naturally abundant and low-cost.¹⁸ Their diameter around $30 \mu\text{m}$ is rather uniform and their spiked structure is evident in electron micrographs (Figure 1C). A further advantage of needle structure is that this offers a large surface area onto which the solid-state fuel can attach. An additional benefit of the $30 \mu\text{m}$ size is that as the Brownian rotational diffusion time is slow for particles of this size, ca. 10^4 s from standard calculations,¹⁹ trajectories are straight or curved only slightly over times significantly less than this time.

■ EXPERIMENTAL SECTION

Solid-State Fuel. The synthesis of DPCP (diphenylcyclopropenone) molecule is described in detail in an earlier paper by one of the authors.²⁰ A typical reprecipitation method was used to grow the microcrystals.²¹ Figure 1D shows an illustrative SEM (scanning electron microscope) image of DPCP microribbons that were precipitated in the absence of motor carriers.

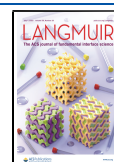
SEM Micrographs. SEM micrographs were taken on a Hitachi S4800 scanning electron microscopy in the user facility of our university.

Microparticles. Defatted pollen grains from the common sunflower (*Helianthus annuus* L.) were purchased from Greer laboratories (NC, USA) and the sunflower sporopollenin exine

Received: May 19, 2020

Revised: June 12, 2020

Published: June 22, 2020



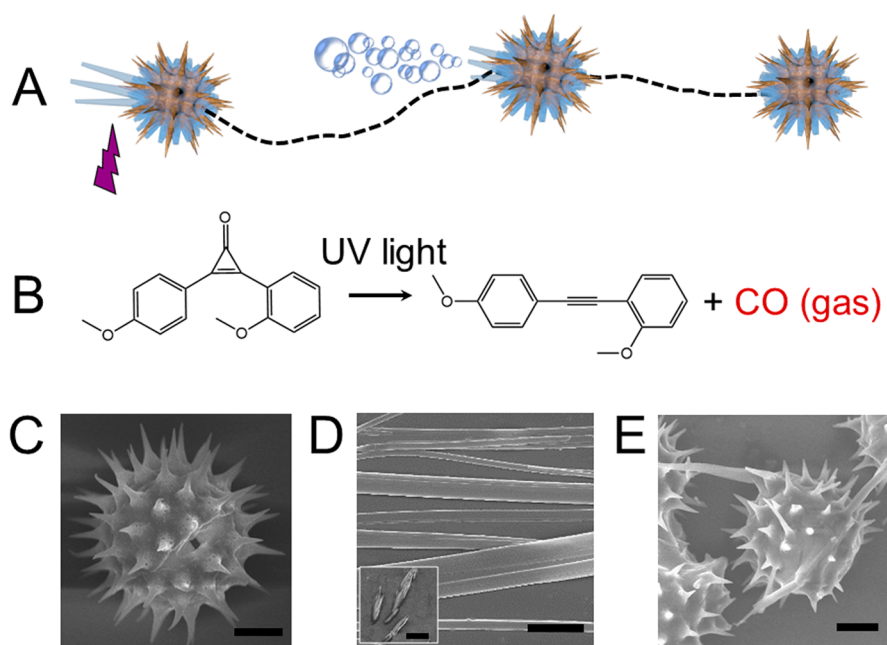


Figure 1. Concept of a micromotor propelled after “ignition” by internal solid-state fuel. (A) Under UV light irradiation, the solid fuel (blue long needles) attached to the microparticle begins to react and generate gas bubbles that propel the particle. Propulsion continues after light is switched off. (B) In the chemical reaction implemented here, solid-state DPCP crystals decompose to yield DPA and gaseous CO. (C) SEM (scanning electron microscope) image of a typical unfunctionalized particle (scale bar 6 μm). (D) SEM image of a typical large DPCP microribbon without microparticle present (scale bar 6 μm); the inset shows typical smaller microribbons (scale bar 2 μm). (E) SEM images of typical microparticle with DPCP crystals on the surface (scale bar 6 μm). The crystals appear as long needles.

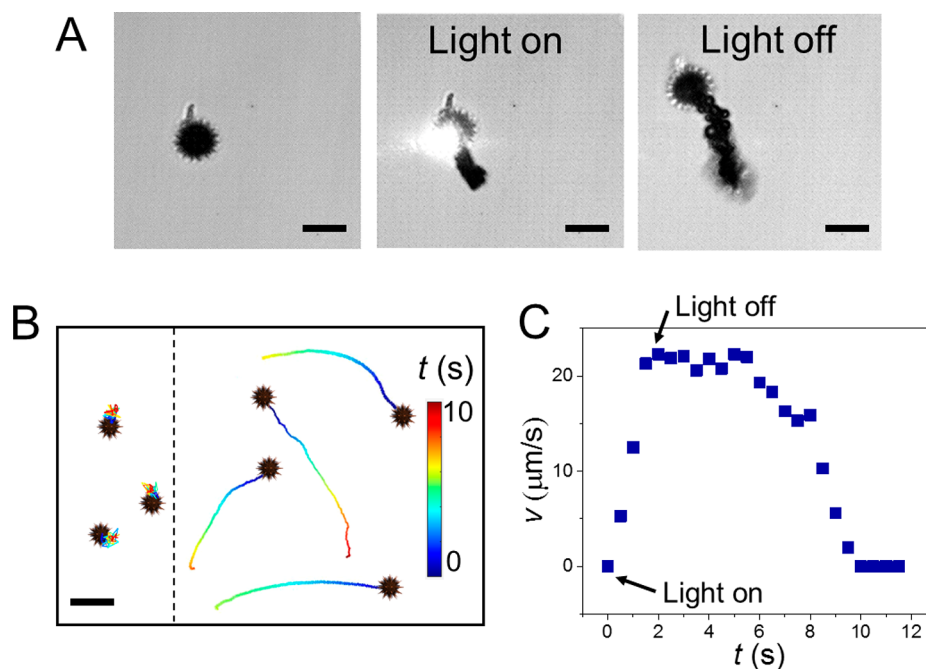


Figure 2. Response to ignition by UV light. (A) Optical image of a microparticle before UV light irradiation (left), during UV light irradiation (middle) and after the trigger light is turned off (right). Ejected gas bubbles are visible owing to the high refractive index difference (scale bar 30 μm). (B) Typical trajectories before UV laser excitation (left panel) and after excitation (right panel) at light intensity 300 mW/cm^2 (scale bar 50 μm). (C) Speed plotted against time for a typical nanoparticle after UV ignition at intensity 300 mW/cm^2 .

capsules were extracted following a literature procedure.¹⁷ Specifically, the pollen grains were suspended in phosphoric acid and mixed to form a homogeneous suspension, which was further heated to 70 $^{\circ}\text{C}$ and stirred gently for 5 h. Then, we collected them by filtration and extensively washed them using water, acetone, hydrochloric acid, and ethanol in sequence. Finally, the extracted capsules were dried at 60 $^{\circ}\text{C}$ for future characterization and experiments.

Loading Fuel onto Microparticles. Quantities of 0.5 mg capsules and 2.5 mg of DPCP powder were mixed in 400 μL of ethanol. The suspension was sonicated for about 2 min. Then 1.0 mL of deionized water was added in one shot, and the mixture was placed still for another 30 min. The liquid became turbid after 30 min with the appearance of small white flocculation, indicating the formation of DPCP crystals. The vial containing the suspension was wrapped in

aluminum foil and stored in a dark cabinet away from exposure to light. The hydrophobic DPCP caused it to crystallize spontaneously onto spikes of the capsules. The rough surface of the microparticles and the high surface to volume ratio further facilitate the attachment process and increase the amount of solid fuel loaded. The SEM micrograph in Figure 1E illustrates needle-like microribbons, indicating that DPCP crystals were attached to the capsules.

UV Excitation to Initiate Propulsion. Into our bright-field imaging system, we integrated a low noise tunable 365 nm UV laser (Thorlabs TCLDM9) whose beam, after passage through a spatial filter and collimation, was focused by a 10× or 20× objective lens onto the sample with a typical spot size around 100 μm . Its on/off state and illumination intensity were controlled by a laser diode controller (Thorlabs LDC 205C).

Bright-Field Imaging of Self-Propelled Particles in Water. Optical videos and images were acquired using a Zeiss Observer Z1 microscope with a 10× objective lens and an EMCCD camera (Andor iXon). Prior to each experiment, 0.5 wt % SDS (sodium dodecyl sulfate) was added to the solution, and the solution was drop cast onto a freshly cleaned glass slide. The images and videos of motor dynamics were processed using the Andor Solis software package, ImageJ (NIH, U.S.A.) and home-built Matlab codes. Individual fuel-loaded capsules were activated by the UV laser and their subsequent motion was tracked.

RESULTS AND DISCUSSION

In these experiments, the analogue of the internal combustion engine is that after reaction is initiated (“ignited”) by UV irradiation, DPCP crystals undergo high-speed photochemical decarbonylation whose mechanism is a chain reaction in which FRET (Förster resonance energy transfer) transfers energy from each product DPA molecule to the neighboring unreacted DPCP molecule in the crystal or between stacked crystals, as the emission spectrum of DPA overlaps the absorption spectrum of unreacted DPCP.²² The cascade reaction is further enabled because the emission energy during the photodissociation of DPCP molecule is higher than that to excite the neighboring DPCP. The chain reaction continues after the UV light is turned off.²⁰ In water, propulsion results from the ejection of bubbles in the form of CO (carbon monoxide) gas.

Our particles, chosen to have a high density (1.8 g/cm³) so that they would sediment to the bottom of our sample cell and be easily tracked by microscopy, migrated in the plane of the cell surface. We observed that the spikes tended to cause frictional drag against the surface; therefore, for particles with less density mismatch from that of the fluid phase, it is reasonable to anticipate propulsion speeds higher than we report below. As noted in the Experimental Section, it was helpful to lower the water surface tension by adding SDS surfactant, as in this environment, the gas bubbles were smaller and detached more rapidly from the capsule surface to give more continuous thrust to the microparticle.²³

Figure 2A illustrates a particle before, during, and after UV irradiation; it is evident that a trail of CO gas continues after the UV light is switched off. Typical trajectories of individual microparticles are shown in Figure 2B, including the cases before and after UV excitation for comparison. It is evident that before launch the particles almost stayed still on this scale of measurement owing to the relatively slow Brownian diffusion of particles this size, but showed active directional motion after triggering until the fuel was consumed. The trajectories are straight or slightly curved paths, as anticipated from the design of this experiment (cf. the Introduction section) to employ particles with a long Brownian

reorientation time. In Figure 2C, the speed of an illustrative particle is plotted against time. One sees acceleration while the UV light is on. When the UV light is switched off, speed remained at a constant level. When the fuel is consumed, the particle decelerates and stops.

We now show that the influence of higher laser trigger intensity was to extend the propulsion lifetime and to increase speed at the same time. In Figure 3, microparticle speed is

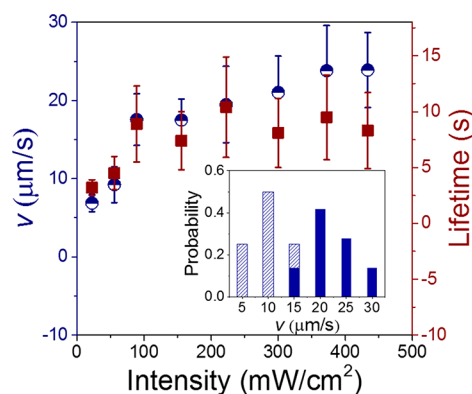


Figure 3. Dependence of particle speed (left ordinate; blue symbols) and lifetime (right ordinate; red symbols) on intensity of UV light in the trigger step. The inset shows the probability distributions of speed at low and high UV trigger intensity, 55 mW/cm² (slash-line columns) and 372 mW/cm² (solid columns), respectively.

plotted against intensity of UV light that triggers the reaction. One sees that the higher the incident intensity, the more energy is transferred in the FRET chain reaction, resulting in a faster generation of bubbles and a larger thrust to increase the motor speed, but less so than linearly. A speed of ca. 7.0 $\mu\text{m}\cdot\text{s}^{-1}$ resulted from the lowest laser intensity (20.0 mW cm⁻²) and it tripled when the laser intensity was increased by a factor of 20. In fact, there is a distribution of speed, probably depending on the density and distribution of solid-state fuel deposited. In Figure 3, the inset shows typical velocity distributions at two different laser intensities, low and high. The propulsion force can be estimated to be from 2.0 pN (~ 20.0 mW cm⁻²) to 6.5 pN (~ 400.0 mW cm⁻²) from the equation $f = \mu v = 6\pi\eta Rv$, where η is the viscosity of the liquid medium (water) and R is the particle radius. This is a lower bound estimate because the motor tends to adhere to the bottom plate due to its high density (~ 1.8 g/cm³) and spiky structure. On the other hand, the trajectory lifetime shows similar increasing trend at low intensity and achieves at a peak value followed by a small subsequent decrease. We suspect that under low illumination intensity conditions the chain reaction cannot consume all of the solid-state fuel, as thermal or radiative decays might terminate the chain at half way,²⁴ while under high illumination the fuel is consumed too quickly. The longest travel distance achieved in these experiments was ca. 400 μm over 20 s, which amounts to 15 times the particle size. The nonmonotonic dependence of the motor lifetime on intensity of the UV trigger suggests that there exists an optimal sweet spot by which to achieve the longest trajectories.

CONCLUSIONS

In conclusion, we have demonstrated a concept to overcome the current limitation that many micromotors require continuous triggering to maintain their propulsion. In a system

with solid-state fuel whose reaction produces ejected gas for propulsion, the chemical chain reaction is triggered by UV light and continues after the UV light is switched off, until the fuel is consumed. With this functionality, the micromotors continue their motion in linear directions without further exposure to the stimulus source, providing new opportunities for micromotor applications in situations where light (or other trigger stimulus) is not desired or possible. Unlike many current methods to produce microparticle propulsion, the chemical reaction propelling these particles does not depend on the surrounding solution, thus enabling the motor to navigate to new environments without concern about the availability of fuel.

Another advantage of this design is that it allows one to selectively activate single micromotors; this is achieved by using a laser trigger spot with size comparable to that of the motor itself. Once ignited, the motor maintains its motion in a linear direction and moves away from the ignition spot without need for light to follow its path; this points to the possibility of accomplishing multitasks using a single system. Probably the greatest current limitation of the present micromotor design is that fuel cannot be reloaded. To accomplish this, the most straightforward path would be to regenerate fuel by growth of new solid DPCP, but this process would be slow. Another approach will be to design specific ligand–receptor binding for attaching pregrown crystals onto microparticles thereby loading new fuel. In future work, the pathway is clear to explore reloading techniques and to optimize the amount of fuel loaded to prolong the propulsion time and to test applications. This concept of an autonomous micromotor can be extended to other fuel chemistries.

AUTHOR INFORMATION

Corresponding Author

Steve Granick – Center for Soft and Living Matter, Institute for Basic Science (IBS), Ulsan 44919, South Korea; Departments of Chemistry and Physics, Ulsan National Institute of Science and Technology (UNIST), Ulsan 44919, South Korea;
✉ orcid.org/0000-0003-4775-2202; Email: sgranick@gmail.com

Authors

Ruo-Yu Dong – Center for Soft and Living Matter, Institute for Basic Science (IBS), Ulsan 44919, South Korea

Yifan Zhang – Center for Soft and Living Matter, Institute for Basic Science (IBS), Ulsan 44919, South Korea; Department of Chemistry, University of Victoria, Victoria, British Columbia V8P 5C2, Canada

Kai Lou – Center for Soft and Living Matter, Institute for Basic Science (IBS), Ulsan 44919, South Korea

Complete contact information is available at:

<https://pubs.acs.org/10.1021/acs.langmuir.0c01486>

Author Contributions

[†]R.-Y.D. and Y.Z. contributed equally.

Notes

The authors declare no competing financial interest.

ACKNOWLEDGMENTS

This work was supported by the taxpayers of South Korea through the Institute for Basic Science, Project Code IBS-R020-D1.

REFERENCES

- (1) Fernández-Medina, M.; Ramos-Docampo, M. A.; Hovorka, O.; Salgueiriño, V.; Städler, B. Recent Advances in Nano- and Micromotors. *Adv. Funct. Mater.* **2020**, *30* (12), 1908283.
- (2) Wang, W.; Duan, W.; Ahmed, S.; Mallouk, T. E.; Sen, A. Small Power: Autonomous Nano- and Micromotors Propelled by Self-Generated Gradients. *Nano Today* **2013**, *8* (5), 531–534.
- (3) Karshalev, E.; Esteban-Fernández De Ávila, B.; Wang, J. Micromotors for “Chemistry-on-the-Fly”. *J. Am. Chem. Soc.* **2018**, *140* (11), 3810–3820.
- (4) Peng, F.; Tu, Y.; Wilson, D. A. Micro/Nanomotors towards in Vivo Application: Cell, Tissue and Biofluid. *Chem. Soc. Rev.* **2017**, *46* (17), 5289–5310.
- (5) Soler, L.; Sánchez, S. Catalytic Nanomotors for Environmental Monitoring and Water Remediation. *Nanoscale* **2014**, *6* (13), 7175–7182.
- (6) Dong, R.; Cai, Y.; Yang, Y.; Gao, W.; Ren, B. Photocatalytic Micro/Nanomotors: From Construction to Applications. *Acc. Chem. Res.* **2018**, *51* (9), 1940–1947.
- (7) Dey, K. K.; Bhandari, S.; Bandyopadhyay, D.; Basu, S.; Chattopadhyay, A. The PH Taxis of an Intelligent Catalytic Microbot. *Small* **2013**, *9* (11), 1916–1920.
- (8) Pacheco, M.; Jurado-Sánchez, B.; Escarpa, A. Visible-Light-Driven Janus Microvehicles in Biological Media. *Angew. Chem., Int. Ed.* **2019**, *58* (50), 18017–18024.
- (9) Wang, J.; Xiong, Z.; Zhan, X.; Dai, B.; Zheng, J.; Liu, J.; Tang, J. A Silicon Nanowire as a Spectrally Tunable Light-Driven Nanomotor. *Adv. Mater.* **2017**, *29* (30), 1701451.
- (10) Zhou, C.; Chen, X.; Han, Z.; Wang, W. Photochemically Excited, Pulsating Janus Colloidal Motors of Tunable Dynamics. *ACS Nano* **2019**, *13* (4), 4064–4072.
- (11) Palacci, J.; Sacanna, S.; Steinberg, A. P.; Pine, D. J.; Chaikin, P. M. Living Crystals of Light-Activated Colloidal Surfers. *Science (Washington, DC, U. S.)* **2013**, *339* (6122), 936–940.
- (12) Pavlick, R. A.; Sengupta, S.; McFadden, T.; Zhang, H.; Sen, A. A Polymerization-Powered Motor. *Angew. Chem., Int. Ed.* **2011**, *50* (40), 9374–9377.
- (13) Li, J.; Yu, X.; Xu, M.; Liu, W.; Sandraz, E.; Lan, H.; Wang, J.; Cohen, S. M. Metal–Organic Frameworks as Micromotors with Tunable Engines and Brakes. *J. Am. Chem. Soc.* **2017**, *139* (2), 611–614.
- (14) Patiño, T.; Arqué, X.; Mestre, R.; Palacios, L.; Sánchez, S. Fundamental Aspects of Enzyme-Powered Micro- and Nanoswimmers. *Acc. Chem. Res.* **2018**, *51* (11), 2662–2671.
- (15) Wang, J.; Xiong, Z.; Liu, M.; Li, X.; Zheng, J.; Zhan, X.; Ding, W.; Chen, J.; Li, X.; Li, X. D.; Feng, S.-P.; Tang, J. Rational Design of Reversible Redox Shuttle for Highly Efficient Light-Driven Microswimmer. *ACS Nano* **2020**, *14* (3), 3272–3280.
- (16) Bahng, J. H.; Yeom, B.; Wang, Y.; Tung, S. O.; Hoff, J. D.; Kotov, N. Anomalous Dispersions of ‘Hedgehog’ Particles. *Nature* **2015**, *517* (7536), 596–599.
- (17) Wang, H.; Potroz, M. G.; Jackman, J. A.; Khezri, B.; Marić, T.; Cho, N. J.; Pumera, M. Bioinspired Spiky Micromotors Based on Sporopollenin Exine Capsules. *Adv. Funct. Mater.* **2017**, *27* (32), 1702338.
- (18) Maric, T.; Nasir, M. Z. M.; Rosli, N. F.; Budanović, M.; Webster, R. D.; Cho, N.; Pumera, M. Microrobots Derived from Variety Plant Pollen Grains for Efficient Environmental Clean Up and as an Anti-Cancer Drug Carrier. *Adv. Funct. Mater.* **2020**, *30*, 2000112.
- (19) Kapral, R. Perspective: Nanomotors without Moving Parts That Propel Themselves in Solution. *J. Chem. Phys.* **2013**, *138* (2), 020901.
- (20) Gong, Y.; Zhang, Y.; Xiong, W.; Zhang, K.; Che, Y.; Zhao, J. Molecular Interactions Control Quantum Chain Reactions toward Distinct Photoresponsive Properties of Molecular Crystals. *J. Am. Chem. Soc.* **2017**, *139* (31), 10649–10652.
- (21) Kasai, H.; Nalwa, H. S.; Oikawa, H.; Okada, S.; Matsuda, H.; Minami, N.; Kakuta, A.; Ono, K.; Mukoh, A.; Nakanishi, H. A Novel

Preparation Method of Organic Microcrystals. *Jpn. J. Appl. Phys.* **1992**, 31, L1132–L1134.

(22) Takeuchi, S.; Tahara, T. Femtosecond Absorption Study of Photodissociation of Diphenylcyclopropanone in Solution: Reaction Dynamics and Coherent Nuclear Motion. *J. Chem. Phys.* **2004**, 120 (10), 4768–4776.

(23) Ma, X.; Jang, S.; Popescu, M. N.; Uspal, W. E.; Miguel-López, A.; Hahn, K.; Kim, D.-P.; Sánchez, S. Reversed Janus Micro/Nanomotors with Internal Chemical Engine. *ACS Nano* **2016**, 10 (9), 8751–8759.

(24) Kuzmanich, G.; Gard, M. N.; Garcia-Garibay, M. A. Photonic Amplification by a Singlet-State Quantum Chain Reaction in the Photodecarbonylation of Crystalline Diarylcyclopropanones. *J. Am. Chem. Soc.* **2009**, 131 (32), 11606–11614.